arXiv:0808.3457v2 [nucl-th] 5 Nov 2008

A model comparison of resonance lifetime modifications, a soft equation of state and non-Gaussian effects on $\pi - \pi$ correlations at FAIR/AGS energies

Qingfeng Li [1,2*] and Marcus Bleicher, [3]

1) Frankfurt Institute for Advanced Studies (FIAS),

Johann Wolfgang Goethe-Universität, Max-von-Laue-Str. 1,

D-60438 Frankfurt am Main, Germany

2) School of Science, Huzhou Teachers College, Huzhou 313000, China

3) Institut für Theoretische Physik,

Johann Wolfgang Goethe-Universität, Max-von-Laue-Str. 1,

D-60438 Frankfurt am Main, Germany

4) Gesellschaft für Schwerionenforschung (GSI),

Planckstr. 1, D-64291 Darmstadt, Germany

Abstract

HBT correlations of $\pi^- - \pi^-$ pairs at FAIR/AGS energies are investigated by using the UrQMD transport model and the CRAB analyzing program. Three different possible sources (treatment of resonance lifetimes, a soft equation of state and non-Gaussian effects) to understand the HBT R_O/R_S puzzle are investigated. Firstly, we find that different treatments of the resonance decay time can not resolve the HBT time-related puzzle, however it can modify the HBT radii at low transverse momenta to some extent to explain the data slightly. Secondly, with a soft equation of state with momentum dependence, the measured transverse momentum dependent HBT radii and R_O/R_S ratio can be described fairly well. Thirdly, non-Gaussian effects are visible in the calculated correlation function. Using the Edgeworth expansion, one finds that the non-Gaussian effect is strongest in the longitudinal direction and weakest in the sideward direction.

(Some figures in this article are in colour only in the electronic version)

* E-mail address: liqf@fias.uni-frankfurt.de

I. INTRODUCTION

It is well-known that one can extract information on the space-time dimensions of the particle emission source (the region of homogeneity) in heavy-ion collisions (HICs) by using the Hanbury-Brown-Twiss interferometry (HBT) [1, 2, 3] techniques. With the ongoing advances in detectors and accelerators one is able to explore collision energies for HICs from less than $\sqrt{s_{NN}} \sim 2.5$ GeV (SIS/FAIR energy regime), $2.5 - 20$ GeV (FAIR/AGS and SPS) up to $20 - 200$ GeV (RHIC). Within this broad energy region Quantum Chromodynamics (QCD) predicts a transition from a hadron gas to a quark-gluon plasma (QGP), and it is expected that this new QGP state of matter exists at least temporarily in the center of HICs. During the phase transition (i.e., in the mixed phase), it was proposed that a nontrivial transition in the spatio-temporal characteristics of the source exists [4]. Unfortunately, so far the excitation functions of the HBT parameters have not shown any *obvious* discontinuities in experiments with energies from SIS, AGS, SPS, up to RHIC [6]. Instead, several unexpected and interesting phenomena occurred, namely, the "E-puzzle", the "t-puzzle", and the "non-Gaussian" effect [5, 6, 7, 8] (for an explanation of these terms, see below). Objectively speaking, the existing theoretical investigations are still in-sufficient and further thorough investigations are needed.

In a recent work on the HBT correlation, adopting the Ultra-relativistic Quantum Molecular Dynamics (UrQMD, v2.2) transport model [9, 10, 11] and the "correlation after-burner" (CRAB, v3.0β) analyzing program [12, 13, 14], the transverse momentum, system-size, centrality, and rapidity dependence of the HBT parameters of the sources of different identical particle pairs (two πs, two Ks, and two Λs) at AGS, SPS and RHIC energies [7, 15, 16, 17, 18] were investigated. It was found that although the calculations are generally in line with the experimental data, discrepancies are not negligible. One of the most puzzling phenomena is that the calculated ratio of HBT radii in the outward direction (R_O) and in sideward direction (R_S) from central HICs is always larger than that extracted from the data at all investigated energies, if the cascade mode is employed, which was named as the HBT time-related puzzle ("HBT t-puzzle") [7]. After considering a soft equation of state (EoS) with momentum dependence (dubbed as SM-EoS) for formed baryons and a simple Skyrme-like (density dependent) potential for the "pre-formed" particles [15], the HBT radius R_O is pushed down and the R_S is pulled up to approach the data so that the "HBT t-puzzle"

disappears throughout the whole energy region. Meanwhile, the transverse mass (m_T) scaling, which was predicted in Ref. [19], and has been probed by several experiments recently [6, 20], can also be much better understood with the help of "pre-formed" particle potentials in HICs [16]. Therefore, it was concluded that the interaction (here it is embodied with potentials) of particles at the early stages of HICs can help to solve the "HBT t-puzzle".

However, besides the potential effects, the resonance dynamics and decay may also influence the momentum distribution of emitted particles as well as their correlation [8]. Since this question has been left aside in our previous works, in this paper, we want to complete the discussion by investigating the effects of the handling of resonance decay times on the HBT quantities by adopting the microscopically transport model UrQMD. The different contributions from the resonance decay and from the potential modification are then compared. In order to have a clearer situation, in this paper we restrict ourselves to the low energy region, i.e., the FAIR/AGS energy regime. In this energy region hadronic interactions dominate the dynamics. String dynamics is negligible and the quarks are still confined and the interactions between them do not need to be taken into account during the HICs. A further simplification is that the available resonances at these beam energies are mainly the $\Delta(1232)$s, and one can restrict the analysis of resonance modification to this hadron. Due to the fact that pions have the largest abundance, they are well suited for the present analysis. Negatively charged pions can be easily measured (no contamination from misidentified K^+s and protons) and experimental data are therefore available from most experiments today. Thus, we focus the present analysis on negatively charged pions.

The paper is arranged as follows. In the next section, the UrQMD transport model and the CRAB analyzing program are introduced. The different treatments of Δ decay and the effects on pion production are also discussed. In Section 3, firstly, the Gaussian fitting to the one- and the three-dimensional correlation functions of negatively charged pions and the non-Gaussian effect are explored and discussed. Secondly, we show the comparison of the transverse momentum dependence of HBT radii and R_O/R_S ratios (from the Gaussian fitting) between calculations with different treatments of the resonance decay and with(without) mean field potentials and experimental data at AGS energies. Finally, in section 4, a summary and outlook is given.

II. MODELS AND TREATMENTS

A. UrQMD transport model

The first formal version (ver1.0) of the UrQMD transport model was published in the end of last century [9, 10, 21]. Since then, a large number of successful theoretical analyses, predictions, and comparisons with data based on this transport model have been accomplished for *pp*, *p*A and AA reactions for a large range of beam energies, i.e., from SIS, AGS, SPS, up to RHIC [22].

The UrQMD model is based on analogous principles as the Quantum Molecular Dynamics model (QMD) [23, 24] and the Relativistic Quantum Molecular Dynamics model (RQMD) [25]. Similar to QMD, hadrons are represented by Gaussian wave packets in phase space, and the phase space of hadron i is propagated according to Hamilton's equation of motion:

$$\dot{\mathbf{r}}_i = \frac{\partial H}{\partial \mathbf{p}_i}, \qquad \text{and} \qquad \dot{\mathbf{p}}_i = -\frac{\partial H}{\partial \mathbf{r}_i}. \tag{1}$$

Here $\mathbf{r}$ and $\mathbf{p}$ are the coordinate and momentum of hadron i. The Hamiltonian H consists of the kinetic energy T and the effective two-body interaction potential energy V,

$$H = T + V, \tag{2}$$

and

$$T = \sum_i (E_i - m_i) = \sum_i (\sqrt{m_i^2 + \mathbf{p}_i^2} - m_i). \tag{3}$$

In the standard version of UrQMD model [9, 10, 21], the potential energies include the two-body and three-body (which can be approximately written in the form of two-body interaction) Skyrme- (also called as the density dependent terms), Yukawa-, Coulomb-, and Pauli-terms as a base.

$$V = V_{sky}^{(2)} + V_{sky}^{(3)} + V_{Yuk} + V_{Cou} + V_{Pau}. \tag{4}$$

And the single particle potential follows from $U = \delta V/\delta f$, where f is the phase space distribution function which reads as

$$f(\mathbf{r}, \mathbf{p}) = \sum_i f_i(\mathbf{r}, \mathbf{p}) = \sum_i \frac{1}{(\pi\hbar)^3} e^{-(\mathbf{r}-\mathbf{r}_i)^2/2L^2} e^{-(\mathbf{p}-\mathbf{p}_i)^2 \cdot 2L^2/\hbar^2}, \tag{5}$$

here L is the width parameter of the wave packet. Recently, in order to be more successfully applied into the intermediate energy region ($0.1 \lesssim E_b \lesssim 2$A GeV), the UrQMD has contained more potential terms [26], those are, 1) the density-dependent symmetry potential, which is essential for isospin-asymmetric reactions at intermediate and low energies, and 2) the momentum-dependent term [27]

$$U_{md} = t_{md} \ln^2[1 + a_{md}(\mathbf{p}_i - \mathbf{p}_j)^2]\rho_i/\rho_0, \tag{6}$$

where t_{md} and a_{md} are parameters, ρ_0 is the normal density. ρ_i is the density of the baryon i,

$$\rho_i = \int \rho(\mathbf{r_i})\rho \mathbf{dr} = \int \rho(\mathbf{r_i}) \sum_{\mathbf{j}} \rho(\mathbf{r_j}) \mathbf{dr} = \frac{\mathbf{1}}{(\mathbf{4\pi L})^{\mathbf{3/2}}} \sum_{\mathbf{j}} \mathbf{e}^{-\frac{(\mathbf{r_i}-\mathbf{r_j})^{\mathbf{2}}}{\mathbf{4L}}}. \tag{7}$$

With these updates, some sensitive probes of the (density dependent) symmetry potential have been proposed [26, 28, 29, 30]. Further, it was also found that the experimental pion and proton directed and elliptic flows from HICs with beam energies from ~ 100A MeV to 2A GeV can be well described [31].

At higher beam energies, the Yukawa-, Pauli-, and symmetry- potentials of baryons becomes negligible, while the Skyrme- and the momentum-dependent part of potentials still influence the whole dynamical process of HICs. With the help of a covariant prescription of mean field from RQMD/S [32], the effects of the mean field with momentum dependence on collective flows from HICs at 2-158A GeV energies were studied by a Jet AA Microscopic Transportation Model (JAM) and it has been found that the momentum dependence in the nuclear mean field is important for the understanding of the proton collective flows at AGS and even at SPS energies [33]. In this work, we choose the same SM-EoS as that in Ref. [33], where the momentum dependent term reads as

$$U_{md} = \sum_{k=1,2} \frac{t^k_{md}}{\rho_0} \int d\mathbf{p}_j \frac{f(\mathbf{r}_i, \mathbf{p}_j)}{1 + [(\mathbf{p}_i - \mathbf{p}_j)/a^k_{md}]^2}, \tag{8}$$

where the U_{md} consists of two parts with separate parameters in order to fit better the real part of the optical potential [34]. We found that the momentum dependent term is also important to explain the transverse momentum dependence of the HBT parameters at AGS energies [15, 35]. Furthermore, as in Ref. [33], the relativistic effects on the relative distance $\mathbf{r}_{ij} = \mathbf{r}_i - \mathbf{r}_j$ and the relative momentum $\mathbf{p}_{ij} = \mathbf{p}_i - \mathbf{p}_j$ employed in the two-body potentials (Lorentz transformation) are considered as follows:

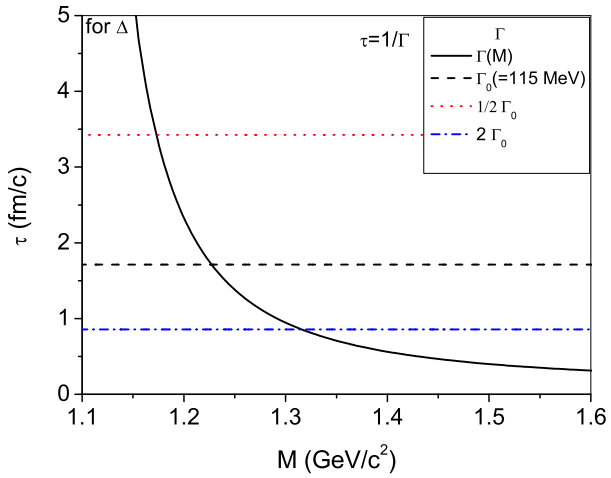

FIG. 1: Lifetime τ of the $\Delta(1232)$ resonance defined as the inverse of resonance width. 1/2, 1, and 2 times of $\Delta(1232)$ width at the pole mass are selected as well as a mass dependent one ($\Gamma(M)$).

$$\tilde{\mathbf{r}}_{\mathbf{ij}}^{\mathbf{2}} = \mathbf{r}_{ij}^2 + \gamma_{ij}^2(\mathbf{r}_{ij} \cdot \beta_{ij})^2, \tag{9}$$

$$\tilde{\mathbf{p}}_{\mathbf{ij}}^{\mathbf{2}} = \mathbf{p}_{ij}^2 - (E_i - E_j)^2 + \gamma_{ij}^2(\frac{m_i^2 - m_j^2}{E_i + E_j})^2. \tag{10}$$

In Eqs. 9 and 10 the velocity factor β_{ij} and the corresponding γ-factor of i and j particles are defined as $\beta_{ij} = (\mathbf{p}_i + \mathbf{p}_j)/(E_i + E_j)$ and $\gamma_{ij} = 1/\sqrt{1 - \beta_{ij}^2}$.

A covariance-related reduction factor for potentials in the Hamiltonian, m_j/E_j, was introduced in the simplified version of RQMD model [32] and adopted in this work as well.

The collision term of the UrQMD model treats 55 different baryon species (including nucleon, Δ, Λ, Σ, Ξ, and Ω and their resonances with masses up to 2.25 GeV) and 32 different meson species (including light unflavored and strange mesons and their resonances with masses up to 2.0 GeV) as tabulated in the PDG [36]. Through baryon-antibaryon symmetry the respective antibaryons are included. The isospin is explicitly treated as well [9, 10]. For hadronic continuum excitations a string model is used. Starting from the version 2.0, the PYTHIA is incorporated into UrQMD in order to investigate the jet production and fragmentation at RHIC energies [11].

B. Treatments of the Δ resonance decay in UrQMD

The frequently used approach to resonance lifetimes in most transport calculations is the application of $\tau = 1/\Gamma$ in conjunction with a Monte-Carlo sampling of the exponential decay law. The decay width Γ of a resonance is usually either taken to be constant (Γ_0) or mass dependent ($\Gamma(M)$) [9, 10]. Fig. 1 shows the lifetimes of the $\Delta(1232)$ resonance as a function of its invariant mass. Considering that the spectral functions might be modified (width and the position of the mass pole) by the hot and dense nuclear medium - e.g., recently a precision measurement of low-mass muon pairs in 158A GeV Indium-Indium collisions at the CERN-SPS was reported, and the associated space-time averaged ρ-meson spectral function shows a strong broadening, but essentially no shift in mass [54] - it is desirable to explore the effect of the broadening/narrowing of resonances on pion freeze-out. Therefore, two other mass-independent lifetimes for $\Delta(1232)$ are adopted which correspond to the widths $1/2\Gamma_0$ and $2\Gamma_0$, respectively (shown also in Fig. 1). The lifetimes of other resonances are not altered in the calculations.

It should be noted that the treatment of the resonance lifetimes and widths in a medium is a long standing problem and much argued in the theory community. In fact, the widely used prescription for resonance lifetimes (especially for broad resonances) in transport models are still under debate. Especially, the recent definition of the lifetime by the derivative of phase shift with respect to the center-of-mass energy is thought to be more reasonable [38, 39, 40]. However, there still exist difficulties to adopt the "new" lifetime *consistently* in transport models. In addition, as a result of the scattering, the forward going part of the wave packet can suffer a different time delay from the scattered one, which is not trivial to implement, and, it is still not understood how to tackle the issue of negative time delay in the real transport model calculations [9, 38]. Due to this ongoing debate, we stick to the above mentioned schematic change by factors of 2 to see if any effect emerges from this modification at all.

Fig. 2 (upper plots) depicts transverse mass spectra of charged pions at midrapidity ($|Y_{cm}| < 0.05$, $Y_{cm} = \frac{1}{2}\log(\frac{E_{cm}+p_\parallel}{E_{cm}-p_\parallel})$, E_{cm} and $p_\parallel$ are the energy and longitudinal momentum of the pion in the center-of-mass system) for central ($< 5\%$ σ_T) Au+Au collisions at 2A GeV. The lower plot shows the ratio between π^- and π^+ transverse mass spectra. The data are taken from Ref. [41]. The lines correspond to calculations with and without potentials

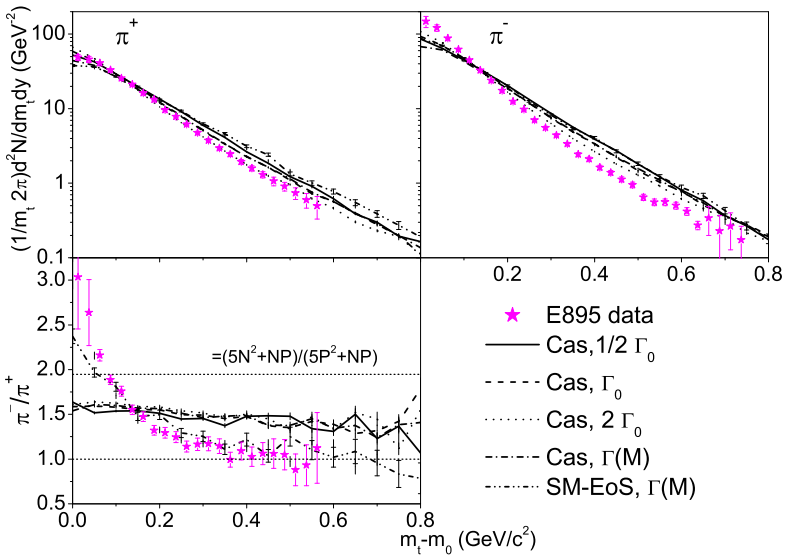

FIG. 2: Upper plots: Charged pion transverse mass spectra at midrapidity ($|Y_{cm}| < 0.05$) for central ($< 5\%$ σ_T) Au+Au collisions at 2A GeV. Lower left plot: The ratio between π^- and π^+ transverse mass spectra. The calculations with various lifetimes in cascade mode ("Cas") as well as in potential mode ("SM-EoS") are compared with the E895 data [41]. The horizontal lines represent the unity and the value $(5N^2 + NP)/(5P^2 + NP)$, separately (see text).

(the "SM-EoS" and the "Cas" modes), as well as calculations with mass-dependent lifetimes for all resonances (with respect to "$\Gamma(M)$") and with three mass-independent lifetimes for $\Delta(1232)$ resonance (with respect to $1/2\Gamma_0^\Delta$, Γ_0^Δ, and $2\Gamma_0^\Delta$, respectively) while other particles are not changed. In line with the previous UrQMD calculations [11], the π transverse mass spectrum can be well described by the cascade calculation, except for a slight deviation from the data at large transverse masses. It is found that a broader constant width of the $\Delta(1232)$ resonance makes the spectra a little steeper since the Δ resonances decay earlier. The mass dependence of the resonance lifetime only influences slightly the spectra in the low transverse mass region, which is mainly due that the Δ resonances with their relatively small masses have long lifetimes, as a consequence, have a higher probability to be absorbed through the $N\Delta \rightarrow NN$ detailed balance process. However, it is interesting to see in the lower plot of Fig. 2 that the ratio between π^- and π^+ spectra is reproduced fairly well with the "SM-EoS" mode, while there is no transverse mass dependence in the cascade modes. The value $(5N^2 + NP)/(5P^2 + NP)$ ("N" and "P" represent the initial neutron and proton

numbers of HICs) of the horizontal line is obtained if only the single pion production via Δ resonances in nucleon-nucleon collisions is considered. However, the effects of such as potentials, reabsorptions, and rescatterings of pions, Δs, and other resonances will change the value visibly. The strong transverse mass dependence of the π^-/π^+ ratio observed in this plot is mainly due to the Coulomb interaction between charged particles which has been investigated before [26, 27, 30, 42, 43].

C. CRAB analyzing program and the fitting process

To calculate the two-particle correlator, the CRAB program is adopted [14], which is based on the formula:

$$C(\mathbf{k},\mathbf{q}) = \frac{\int d^4x_i d^4x_j g(x_i,p_i) g(x_j,p_j) |\phi(\mathbf{r}',\mathbf{q}')|^2}{\int d^4x_i g(x_i,p_i) \int d^4x_j g(x_j,p_j)}. \tag{11}$$

Here $g(x_i,p_i)$ is an effective probability for emitting a particle i with 4-momentum $p_i = (E_i,\mathbf{p}_i)$ from the space-time point $x_i = (t_i,\mathbf{r}_i)$. $\phi(\mathbf{r}',\mathbf{q}')$ is the relative wave function with $\mathbf{r}'$ being the relative position in the pair's rest frame. $\mathbf{q} = \mathbf{p}_i - \mathbf{p}_j$ and $\mathbf{k} = (\mathbf{p}_i + \mathbf{p}_j)/2$ are the relative momentum and the average momentum of the two particles i and j. Due to the quantum statistics, the correlator is larger than unit at small q for bosons, and in the absence of strong and Coulomb final state interactions, the wave function of an identical pair of bosons reads as

$$|\phi(\mathbf{r}',\mathbf{q}')|^2 = 1 + \cos(2\mathbf{q}'\cdot\mathbf{r}'). \tag{12}$$

And the two-particle correlator and the "region of homogeneity" can be directly related by a Fourier transformation. However, in HICs, the Coulomb and strong interactions might distort the wave function and the direct relationship between the correlator and the region of homogeneity disappears. As a standard method, one can fit the correlator as a three-dimensional (3D) Gaussian form under various reference frames, in which the longitudinal comoving system (LCMS) (or called as the "Out-Side-Long" system) is more frequently adopted in recent years. We use it in the present work as well. The corresponding 3D Gaussian correlation function can be expressed as

$$C(q_O,q_S,q_L) = K[1 + \lambda \exp(-R_L^2 q_L^2 - R_O^2 q_O^2 - R_S^2 q_S^2 - 2R_{OL}^2 q_O q_L)]. \tag{13}$$

In Eq. 13 the K is the overall normalization factor, the q_x and R_x are the components of the pair relative momentum and homogeneity length (HBT radius) in the x direction, respectively. The λ parameter is commonly called the incoherence factor and lies between 0 (complete coherence) and 1 (complete incoherence) for bosons in realistic HICs. Because the parameter λ might be influenced by many additional factors, such as contamination, long-lived resonances, or the details of the Coulomb modification in the FSI, we regard it as a free parameter. The R_{OL}^2 represents the cross-term and plays a role at large rapidity [8, 17, 44].

However, due to the resonance decay and the space-time correlation [45, 46, 47], the emission function has been found to deviate from a Gaussian form (the non-Gaussian effect). In order to gain clearer information about the source, both fitting the correlator to a (3-dimensional) Gaussian form with higher orders of a harmonics and the (3-dimensional) imaging technique [48, 49] are available. The high orders of harmonic fitting by the Edgeworth expansion was proposed by Csörgő [50] and used in experiments [51], which is expressed as

$$C(q_{\rm inv}) = K_{\rm inv}[1 + \lambda_{\rm inv}\exp(-R_{\rm inv}^2 q_{\rm inv}^2)][1 + \sum_{n=4,even}^{\infty} \frac{\kappa_{{\rm inv},n}}{n!(\sqrt{2})^n} H_n(R_{\rm inv} q_{\rm inv})]. \qquad (14)$$

Here the subscription "inv" means that the one-dimensional (1D) correlation function is constructed in the invariant quantity $q_{\rm inv} = \sqrt{(q^0)^2 - (\mathbf{q})^2}$ while $R_{\rm inv}$ is the corresponding 1D radius. n is the order parameter, and the H_n reads as

$$H_n(z) = (-1)^n e^{z^2} \frac{d^n}{dz^n} e^{-z^2}. \qquad (15)$$

To calculate the HBT two-pion correlation, firstly, we select central collisions at AGS energies in the UrQMD model: Au+Au at E_b = 2, 4, 6, and 8A GeV (< 11% of the total cross section σ_T), with a rapidity cut $|Y_{cm}| < 0.5$. For each case about 40 thousand events are calculated. All particles with their phase space coordinates at their freeze-out times are put into the CRAB analyzing program. Only the negatively charged pions are considered during the analyzing process in this work (for each analysis, one billion pion pairs are considered). We found that the Coulomb effect in FSI on the HBT radii of the pion source is small [16], so that we do not consider it in the calculations.

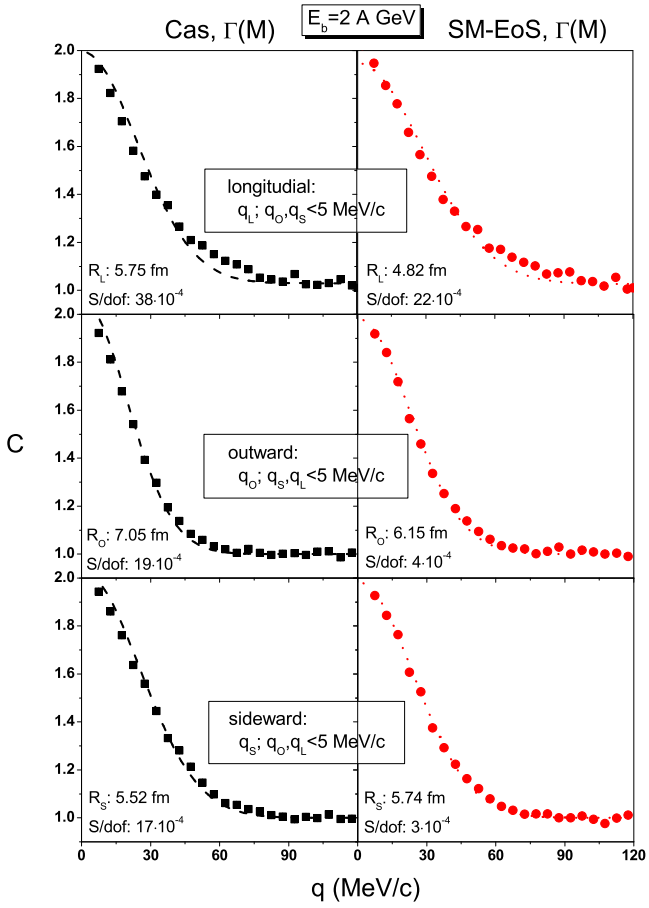

FIG. 3: Projections of the correlation function for negatively charged pions in longitudinal (top plots), outward (middle) and sideward (bottom) directions from central Au+Au collisions at $E_b = 2$ A GeV. The results with "Cas" (left plots) and "SM-EoS" modes (right) are shown with points. The mass-dependent lifetime of resonances is employed in the calculations. 1D Gaussian fit to each projection is shown with lines as well.

III. HBT RESULTS

A. Gaussian fitting

In Fig. 3 we show the projections of the calculated correlation function of the pion source in longitudinal (top plots), outward (middle) and sideward (bottom) directions without ("Cas", squares in left plots) and with ("SM-EoS", circles in right plots) potentials. The mass

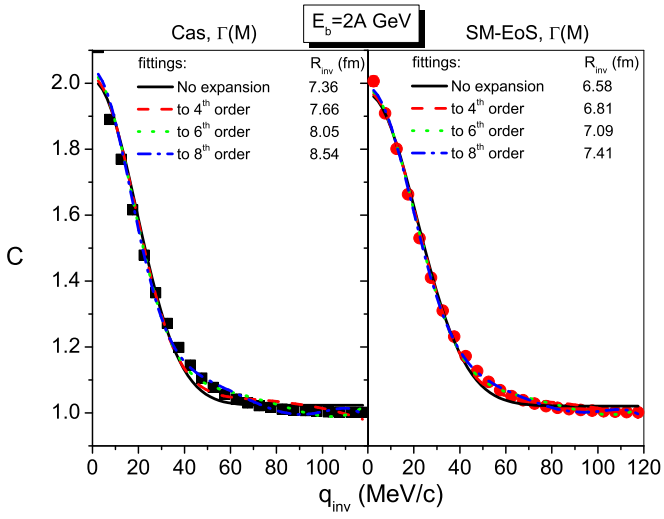

FIG. 4: 1D correlation function for $\pi^-\pi^-$ pairs. Fittings with the Edgeworth expansion up to the eighth order on it are also shown. The result with cascade mode (left plot) is compared to that with the SM-EoS mode (right). The fitting results of the radii $R_{\rm inv}$ are listed in the plots as well.

dependent lifetime of resonances is adopted. Correspondingly, 1D Gaussian fits ($C(q_x) = K_x[1+\lambda_x \exp(-R_x^2 q_x^2)]$ where "x" stands for "L", "O", or "S") to them are also shown with dashed and dotted lines, separately (the values of the HBT radius in each projection and the corresponding reduced least square fit S/dof are also given in each plot). The fitting result shows clearly that the non-Gaussian effect of the correlation function exists especially in the longitudinal direction, while in other two directions it is largely reduced. The Gaussian fitting in the sideward direction is even better than that in the outward direction. We notice that in the data analysis by both the HBT fitting and the imaging method the similar non-Gaussian effect has been observed as well at all AGS, SPS, and RHIC beam energies [51, 52, 53]. The non-Gaussian character originates mainly from both the decay of long- and intermediate-lived resonances, such as η', ω, K^* mesons, and Δ, Λ^*, Σ^* baryons, and the space-time correlation (or flow) effect [45, 46, 47]. At AGS energies, the contributions from meson and hyperon resonances are limited, but the Δ resonance decay plays an important role. The origin of the non-Gaussian effect shown in Fig. 3 might be clear by comparing the HBT results with and without the mean field potential. If comparing the left and the right plots of Fig. 3 roughly, one may find that the Gaussian fitting becomes even better with the consideration of the mean field potential.

To quantitatively analyze the non-Gaussian effect, the Edgeworth expansions up to the 8th order on the 1D correlation function are shown in Fig. 4. It is seen that the $R_{\rm inv}$ increases with the order of the expansion on the correlation function. In the cascade mode, the difference of the $R_{\rm inv}$ values between without expansion and with expansion up to the 8^{th} order reaches 1.18 fm, but in the SM-EoS mode the difference is reduced to 0.83 fm. Similarly, if one takes the same expansions into the long-out-side projections, it is found that, 1) in the cascade mode, the radii in longitudinal, outward, and sideward directions change 2.2, 0.6, and 0.52 fm, respectively. 2) While in the SM-EoS mode, the changes are 1.45, 0.51, and 0.38 fm, respectively. Therefore, the non-Gaussian effect is reduced in all directions of the correlation after considering the mean field potential. Therefore, it is the long- and intermediate-lived resonance decay that mainly contributes to the visible non-Gaussian phenomenon but not the mean field.

B. Transverse momentum dependence of the HBT radii

Fig. 5 gives the transverse momentum k_T ($\mathbf{k}_T = (\mathbf{p}_{1T} + \mathbf{p}_{2T})/2$) dependence of the HBT-radii R_L, R_O, R_S, and the R_O/R_S ratio in central Au+Au collisions at $E_b = 2$A GeV. Experimental data are taken from Ref. [35]. The cascade calculations with mass-independent lifetimes of resonances are shown with different widths of the $\Delta(1232)$ resonance (the widths of other resonances are not changed). With the default width (Γ_0), we find that the radii R_L and R_S are somewhat smaller than the data at small k_T. With a narrower $\Delta(1232)$ width (hence a longer lifetime) the HBT radii at large k_T are increased slightly, and vice versa. This modification can not explain the experimental R_O and R_S data, which can also be clearly seen from their R_O/R_S ratios in the right-bottom plot: the variation of the $\Delta(1232)$ width does not help to obtain a small value of the R_O/R_S ratio as observed in the data.

Comparing the left and the right plots of Fig. 3 more carefully one can find that the mean field potential enhances the incoherence in the reaction plane (x-z plane, correspondingly, the outward-longitudinal plane) but not in the sideward direction. Fig. 6 illustrates the k_T dependent HBT radii R_L, R_O, R_S, and R_O/R_S ratio (from top to bottom plots) of the pion source for the energies $E_b = 2$, 4, 6, and 8A GeV (from left to right plots). With the mass dependent lifetimes for all resonances in the cascade mode ("Cas,$\Gamma(M)$"), the resonances with their small invariant masses decay later and hence expand the source when compared

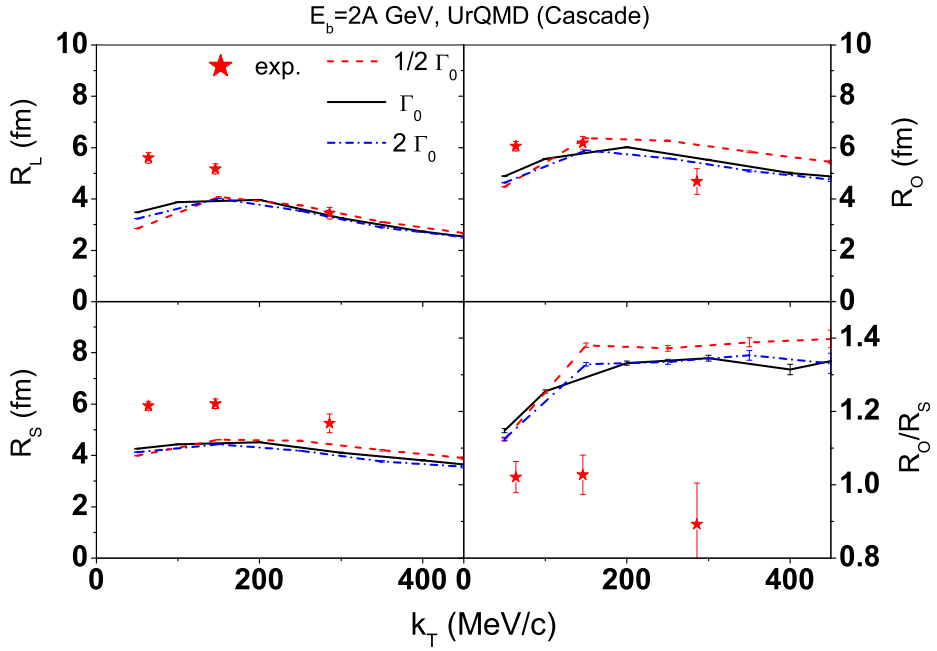

FIG. 5: Transverse momentum k_T dependence of the HBT radii R_L, R_O, R_S, and the R_O/R_S ratio in central Au+Au collisions at $E_b = 2$A GeV. The cascade mode is chosen. The mass-independent lifetime of resonances is considered, while the width of $\Delta(1232)$ resonance is varied from $1/2\Gamma_0$, Γ_0, to $2\Gamma_0$ (the widths of other resonances are not changed). Experimental data are shown [35] with scattered stars.

with the mass-independent lifetime of resonances ("Cas,Γ_0"). Considering the fact that the resonances with small invariant masses tend to produce pions with small momenta, an increase of the HBT radii at small k_T and E_b is understandable. At large k_T as well as at high beam energies, this effect is reduced since less resonances with small invariant masses contribute. It is interesting to see that the result with a mass dependent treatment of resonance lifetimes can match the HBT data better in the AGS energy region. However, it is also seen that the mass dependence will increase the HBT radii with almost equal power in outward and sideward directions and the ratio between R_O and R_S values remains basically unchanged. With the help of the SM-EoS, it is interesting to see that the R_O at large k_T are driven down while the R_S at small k_T are pulled up so that the k_T dependence of the R_O/R_S ratio can be much better described, in line with Ref. [15]. This finding supports that it is the mean field which leads to a stronger phase-space correlation that results in a much better explanation of the HBT time-related puzzle [16].

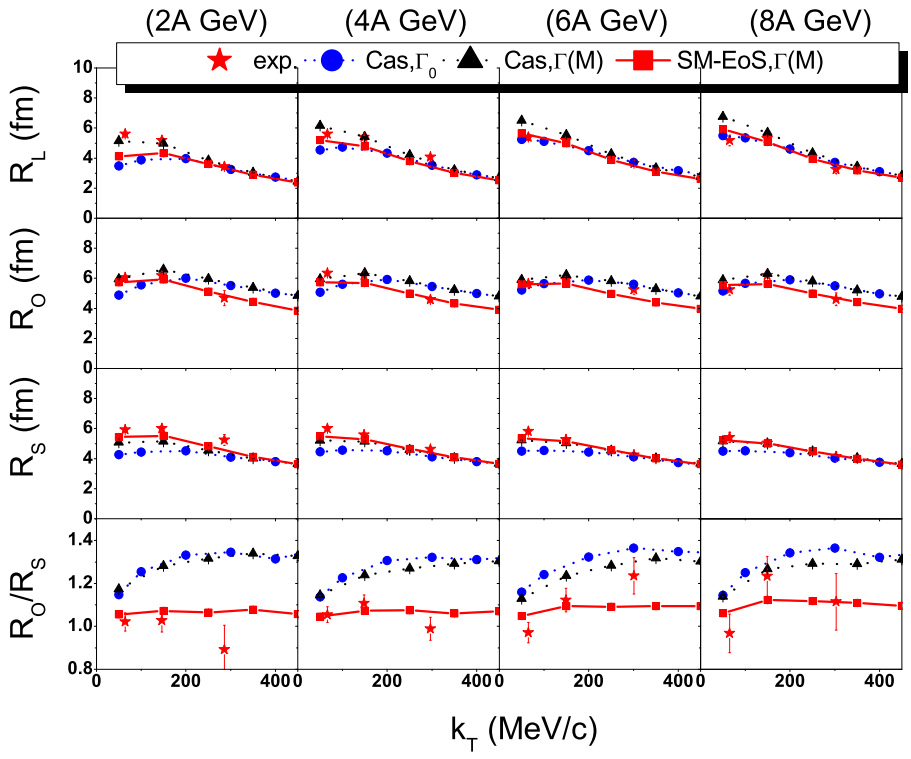

FIG. 6: k_T dependence of HBT radii R_L, R_O, and R_S as well as the R_O/R_S ratio of negatively charged pion source (from top to bottom plots) for central Au+Au collisions at E_b = 2, 4, 6, and 8A GeV (from left to right plots). In calculations, 1) the"Cas,Γ_0" represents the cascade mode with a mass-independent lifetime of resonances. 2) "Cas,$\Gamma(M)$" means the cascade mode with a mass-dependent lifetime of resonances. 3) While the "SM-EoS,$\Gamma(M)$" represents the potential mode with a mass-dependent lifetime of resonances. The experimental data are taken from [35].

IV. SUMMARY AND OUTLOOK

To summarize, the HBT correlation of $\pi^- - \pi^-$ pairs at AGS energies were investigated by using the UrQMD transport model and the CRAB analyzing program. We found that a narrower (wider) width of $\Delta(1232)$ resonance results in larger (smaller) HBT radii in all directions at large k_T, which can not explain the small experimental ratio between R_O and R_S. Although a mass dependent lifetime of the resonances can not resolve this problem as well, but it pulls up the HBT ratii at small k_T and hence slightly improves the HBT radii of pions.

We observed that the k_T dependent HBT radii and R_O/R_S ratio in the AGS energy region

can be described fairly well with a soft equation of state with momentum dependence. This supports the idea that the interaction of particles in the early stage of the reaction (leading to stronger correlation) is the key to solve the HBT time-related puzzle.

Non-Gaussian effects are visible (although weak) in the correlation function and might bring large uncertainties (on the order of ± 1 fm) if the correlation function is fitted only by a Gaussian form. To investigate the non-Gaussian effect, the Edgeworth expansion was used during the fitting process. It was found that the non-Gaussian effect is strongest in the longitudinal direction and weakest in the sideward direction. The decay of the intermediate- and long-lived resonances was found as the main contribution to the non-Gaussian phenomenon, while the mean field potential did not increase this effect.

At higher beam energies, such as SPS and RHIC, the non-Gaussian effects as well as the broadening of vector mesons (in connection to the NA60 results [54]) and its influence on $\pi^+\pi^-$ correlation deserve further investigations. In addition, other, besides pions, (non-)identical particle correlations deserve increased attention as they might provide snapshots of the source geometry at different times of the reaction. These studies are currently underway and will be addressed in a forthcoming paper.

Acknowledgments

We would like to acknowledge support by the Frankfurt Center for Scientific Computing (CSC). This work was supported by the Hessian LOEWE initiative through the Helmholtz International Center for FAIR (HIC for FAIR).

[1] R. Hanbury-Brown and R.Q. Twiss, Philos. Mag. **45**, 663 (1954); Nature (London) **178**, 1046 (1956).

[2] G. Goldhaber, *et al.*, Phys. Rev. **120**, 300 (1960).

[3] W. Bauer, C. K. Gelbke and S. Pratt, Ann. Rev. Nucl. Part. Sci. **42**, 77 (1992).

[4] D. H. Rischke and M. Gyulassy, Nucl. Phys. A **608**, 479 (1996).

[5] S. Soff, S. A. Bass and A. Dumitru, Phys. Rev. Lett. **86**, 3981 (2001).

[6] M. A. Lisa, S. Pratt, R. Soltz and U. Wiedemann, Ann. Rev. Nucl. Part. Sci. **55**, 357 (2005).

[7] Q. Li, M. Bleicher and H. Stöcker, J. Phys. G **34**, 2037 (2007).

[8] U. A. Wiedemann and U. W. Heinz, Phys. Rept. **319**, 145 (1999).

[9] S. A. Bass *et al.*, [UrQMD-Collaboration], Prog. Part. Nucl. Phys. **41**, 255 (1998).

[10] M. Bleicher *et al.*, [UrQMD-Collaboration], J. Phys. G: Nucl. Part. Phys. **25**, 1859 (1999).

[11] E. L. Bratkovskaya *et al.*, Phys. Rev. C **69**, 054907 (2004).

[12] S. E. Koonin, Phys. Lett. B **70**, 43 (1977).

[13] S. Pratt *et al.*, Nucl. Phys. A **566**, 103C (1994).

[14] S. Pratt, 2000, CRAB version 3, http://curly.pa.msu.edu/∼scottepratt/freecodes/crab/home.html.

[15] Q. Li, M. Bleicher and H. Stöcker, Phys. Lett. B **659**, 525 (2008).

[16] Q. Li, M. Bleicher and H. Stöcker, Phys. Lett. B **663**, 395 (2008).

[17] Q. Li, M. Bleicher, X. Zhu and H. Stöcker, J. Phys. G **33**, 537 (2007).

[18] Q. Li, M. Bleicher, and H. Stöcker, Phys. Rev. C **73**, 064908 (2006).

[19] T. Csörgő and B. Lorstad, Phys. Rev. C **54**, 1390 (1996).

[20] I. G. Bearden *et al.* [the NA44 Collaboration], Phys. Rev. Lett. **87**, 112301 (2001).

[21] S. A. Bass *et al.*, Phys. Rev. Lett. **81**, 4092 (1998).

[22] http://th.physik.uni-frankfurt.de/∼urqmd; H. Petersen, M. Bleicher, S. A. Bass and H. Stöcker, arXiv:0805.0567 [hep-ph].

[23] J. Aichelin and H. Stöcker, Phys. Lett. B **176**, 14 (1986).

[24] J. Aichelin, Phys. Rept. **202**, 233 (1991).

[25] H. Sorge, H. Stöcker and W. Greiner, Annals Phys. **192**, 266 (1989).

[26] Q. Li, Z. Li, S. Soff, M. Bleicher and H. Stöcker, J. Phys. G **32**, 151 (2006).

[27] S. A. Bass, C. Hartnack, H. Stöcker and W. Greiner, Phys. Rev. C **51**, 3343 (1995).

[28] Q. Li, Z. Li, S. Soff, M. Bleicher and H. Stöcker, Phys. Rev. C **72**, 034613 (2005).

[29] Q. Li, Z. Li and H. Stöcker, Phys. Rev. C **73**, 051601 (2006).

[30] Q. Li, Z. Li, S. Soff, R. K. Gupta, M. Bleicher and H. Stöcker, J. Phys. G **31**, 1359 (2005).

[31] H. Petersen, Q. Li, X. Zhu and M. Bleicher, Phys. Rev. C **74**, 064908 (2006).

[32] T. Maruyama, K. Niita, T. Maruyama, S. Chiba, Y. Nakahara and A. Iwamoto, Prog. Theor. Phys. **96**, 263 (1996).

[33] M. Isse, A. Ohnishi, N. Otuka, P. K. Sahu and Y. Nara, Phys. Rev. C **72**, 064908 (2005).

[34] S. Hama, B. C. Clark, E. D. Cooper, H. S. Sherif and R. L. Mercer, Phys. Rev. C **41**, 2737 (1990).

[35] M. A. Lisa *et al.* [E895 Collaboration], Phys. Rev. Lett. **84**, 2798 (2000).

[36] C. Amsler *et al.* [Particle Data Group], Phys. Lett. B **667**, 1 (2008).

[54] R. Arnaldi *et al.* [NA60 Collaboration], Phys. Rev. Lett. **96**, 162302 (2006).

[38] P. Danielewicz and S. Pratt, Phys. Rev. C **53**, 249 (1996).

[39] C. David, C. Hartnack and J. Aichelin, Nucl. Phys. A **650**, 358 (1999).

[40] A. B. Larionov, M. Effenberger, S. Leupold and U. Mosel, Phys. Rev. C **66**, 054604 (2002).

[41] J. L. Klay *et al.* [E895 Collaboration], Phys. Rev. C **68**, 054905 (2003).

[42] H. W. Barz, J. P. Bondorf, J. J. Gaardhoje and H. Heiselberg, Phys. Rev. C **57**, 2536 (1998).

[43] J. Barrette *et al.* [E877 Collaboration], Phys. Rev. C **62**, 024901 (2000).

[44] S. Chapman, P. Scotto and U. W. Heinz, Phys. Rev. Lett. **74**, 4400 (1995).

[45] Z. Lin, C. M. Ko and S. Pal, Phys. Rev. Lett. **89**, 152301 (2002).

[46] U. W. Heinz and B. V. Jacak, Ann. Rev. Nucl. Part. Sci. **49**, 529 (1999).

[47] F. Retiere and M. A. Lisa, Phys. Rev. C **70**, 044907 (2004).

[48] D. A. Brown and P. Danielewicz, Phys. Lett. B **398**, 252 (1997).

[49] P. Danielewicz and S. Pratt, Phys. Lett. B **618**, 60 (2005).

[50] T. Csörgő and S. Hegyi, Phys. Lett. B **489**, 15 (2000).

[51] J. Adams *et al.* [STAR Collaboration], Phys. Rev. C **71**, 044906 (2005).

[52] P. Chung and P. Danielewicz, arXiv:0807.4892 [nucl-ex].

[53] S. Y. Panitkin *et al.* [E895 Collaboration], Phys. Rev. Lett. **87**, 112304 (2001).

[54] R. Arnaldi *et al.* [NA60 Collaboration], Phys. Rev. Lett. **96**, 162302 (2006).